

Rapid grain orientation imaging using spatially resolved acoustic spectroscopy

Steve D. Sharples, Matt Clark, Mike G. Somekh, Elizabeth E. Sackett¹, Lionel Germain¹,
Martin A. Bache¹

University of Nottingham, School of Electrical & Electronic Engineering, Nottingham, UK, steve.sharples@nottingham.ac.uk

¹University of Wales Swansea, School of Engineering, Swansea, UK

Abstract: Spatially resolved acoustic spectroscopy (SRAS) is a relatively new technique that can be used to rapidly image the microstructure of metals such as titanium and steel. The ability to image the grain structure and to get an indication of grain orientation is of great interest to many in industries such as aerospace, where anomalous grain structure can have an impact on the mechanical performance of the material.

A fixed-frequency pulsed laser excites surface acoustic waves using a fringe grating whose spacing can be adjusted in real time. Most efficient acoustic excitation - detected using a second laser - occurs when the fringe spacing matches the acoustic wavelength, and in this way the absolute acoustic velocity of the material in the area under the grating can be determined very rapidly. By raster-scanning the sample with respect to the grating and detection point, a velocity map of the sample can be created, revealing the grain structure.

The SRAS technique is noncontact, completely nondestructive, can cope with large samples, and is relatively fast. Velocity images with lateral resolutions approaching 0.4mm, and sensitive to changes in phase velocity of less than 1m/s are presented. Furthermore, by propagating the acoustic waves in more than one direction, an idea of crystal orientation can be determined for individual grains. Images are presented that have been acquired in this manner, and striking comparisons are made with orientation images acquired using electron backscatter diffraction.

Key words: Acoustic imaging, crystal orientation, laser ultrasound, materials characterization.

A. Introduction

The ability to image the microstructure of a material is useful for those studying material properties such as strength and susceptibility to fatigue and failure. For example, techniques such as electron backscatter diffraction (EBSD) - which can determine crystallographic orientation on the surface of the material - have been used to determine that the presence of "quasi-cleavage facets," which determine fatigue crack initiation in the near α and α/β titanium alloys, predominantly form on basal planes of the hexagonal alpha crystallographic phase [1].

For some time, ultrasonic techniques have contributed to the methods used to investigate material

microstructure. The principal contrast mechanism used is the change in ultrasonic phase or velocity, due to grain orientation. This change in velocity can be measured in a number of different ways, and for many years the scanning acoustic microscope (SAM) [2] has been used to produce excellent qualitative images of material microstructure [3]. However, in the SAM's normal mode of operation of imaging, where the leaky surface wave is interfered with the directly reflected wave to give contrast, one does not obtain an image of absolute surface acoustic wave (SAW) velocity. Although it is possible to quantitatively determine the SAW velocity using the $V(z)$ method, to the author's knowledge this has not been attempted previously due to the time it would take to acquire an image. Relatively recent work published has shown it is possible to use a SAM to produce quantitative velocity maps of grain structures using Rayleigh waves [4], and maps relating to residual surface stress using surface skimming longitudinal waves [5], by using a technique based on the difference of arrival times of the direct reflected signal and the surface wave.

Within the past two years a new technique has been described by Sharples, Clark and Somekh [6], [7], termed spatially resolved acoustic spectroscopy (SRAS), for directly and quantitatively imaging the local SAW velocity over the surface of materials. This paper expands on the work of the previous papers by extending the usefulness of the SRAS technique, by combining velocity maps of SAWs propagating in orthogonal directions in order to give some idea of crystallographic orientation.

B. Spatially resolved acoustic spectroscopy

Although the SRAS technique has been described previously [6], [7], it is worth repeating some of the more salient details here for completeness. SRAS is an acoustic technique that has its roots in the optical measurement technique called spectroscopy. The technique itself will be described, and then the instrumentation used to perform the measurements presented in this paper.

SAWs are excited by a fixed frequency source (in the case of our own instrument this is a pulsed laser) using a grating of regularly spaced lines. The spacing of the lines on the grating is swept over a range, likely to correspond to the range of SAW wavelengths at the fixed frequency f for a given material. The SAWs are detected using a broadband detector. The efficiency with which the SAWs are generated in the region of the grating depends on the

line spacing of the fringes.

Fig.1 illustrates the amplitude response of the detected signal as the fringe spacing is swept over a certain range. The largest signal is produced – not surprisingly – when the fringe spacing precisely matches the wavelength of the SAWs, λ , at the excitation frequency in the region of excitation. Since the excitation frequency is fixed, the SAW wavelength is determined by the SAW velocity, v , using the relationship $v = f\lambda$.

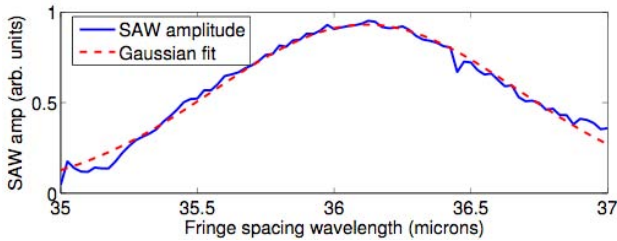


Fig.1. The graph illustrates how the amplitude of the detected SAWs varies as the fringe spacing of the fixed frequency excitation source is varied, in this case between 35 and 37 μm . The largest amplitude occurs when the fringe spacing of the excitation source exactly matches the acoustic wavelength. The solid blue line represents experimental data, the dashed red line is a Gaussian curve fitted to the data.

A small amount of processing would normally be applied to the measured signal, to reduce the effects of the inevitable noise in the measured acoustic amplitude, in order to determine the peak of the amplitude response. In the images shown, we curve-fit to a Gaussian. Although this is not the exact form of curve, it works well because the limited scan range of the fringe spacing means that the “tails” of the response are not present.

The above description illustrates how the velocity for one “point” is calculated, where a “point” corresponds to the area under the grating. To build up a velocity image of the surface of the material, the material must be raster-scanned with respect to the excitation grating and detection point. It is important to note that the calculated velocity corresponds the area under the grating, not to the point at which the SAWs are detected.

C. Instrumentation

The images shown in this paper were acquired using the SRAS technique on our instrument, known as the optical scanning acoustic microscope (O-SAM). The instrument has been described previously [6], [7] and so only the important details will be described for completeness.

The important aspects of the O-SAM system, in its configuration as an instrument for acquiring SAW velocity maps using SRAS, are shown schematically in Fig. 2.

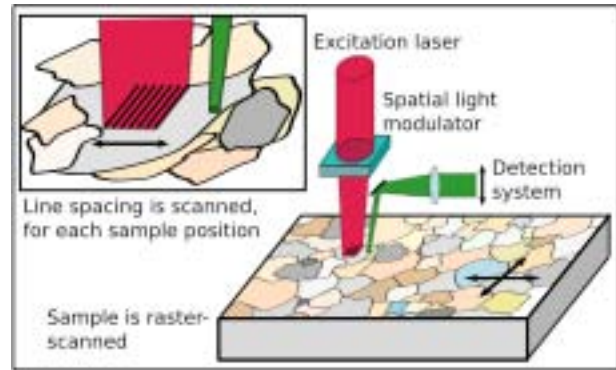


Fig.2. This schematically illustrates the key aspects of the O-SAM, and how it is used to acquire velocity maps using the SRAS technique. The material under investigation is raster scanned with respect to the SAW excitation and detection lasers, and for each sample position the fringe spacing of the excitation pattern is varied using the SLM. The amplitude of the detected SAWs is recorded for each fringe spacing, and from this data the velocity in a certain direction can be determined.

A Q-switched mode locked laser is used to excite the SAWs. At a repetition rate of 1kHz, this laser emits a tone burst of around 30 pulses, each separated from its neighbour by 12.1ns, giving the laser a fundamental frequency of 82MHz. The energy from this pulsed laser is delivered to the material surface via a spatial light modulator (SLM), the pixels of which can be programmed at a rate that matches the Q-switch repetition rate. The SLM is programmed with a pattern of fringes, the spacing of which is varied by the controlling computer in order to collect the data shown in Fig.1 for each point on the sample. The size of the image of the fringes on the material surface is approximately 0.8 x 0.8mm, giving a lateral resolution of around half that.

The SAWs are detected a short distance away from the excitation region. Any of the established techniques for detecting SAWs may be used for this. In the case of the O-SAM instrument, optical beam deflection is used. This technique, although it is simple, robust and inexpensive to use, is sensitive to surface roughness. However it should be noted that other established techniques exist that can be used on rough samples, requiring little or no surface preparation.

The O-SAM acquires the complex amplitude of the acoustic waves at the excitation frequency, at a rate that is limited by the repetition rate of the laser. This means that, although several amplitude measurements are required for each velocity measurement, it is possible to achieve speeds of around 100 velocity measurement points a second, making the technique in general very rapid.

It is important to note that the technique is tolerant to acoustic aberrations, which affect the propagation of the SAWs from excitation region to detection point when propagating through random microstructure [8]. The overall detected amplitude may vary significantly as the sample is scanned from point to point due to the effects of aberrations, however the propagation of SAWs between the edge of the excitation region and the detection point is not affected by a change in fringe spacing. If the excitation region is across two or more

grains, then as the fringe spacing is adjusted the relative generation efficiency within each grain will change. This does affect the properties of the propagating wavefront, but it is a second order effect.

D. Results

The SRAS technique was used to acquire velocity images of two samples, both of which are titanium alloys. The samples were polished before scanning, although again it should be stressed that a good surface finish is only necessary for the particular optical detection technique used in the O-SAM instrument, and is not necessary for the SRAS technique in general.

Fig.3 is of a titanium alloy known as Ti-6246. Parts (a) and (b) of the figure represent the different SAW velocities as different colours, in the range 2700ms^{-1} (dark blue) to 3100ms^{-1} (dark red). In Fig.3a the waves are propagating from left to right, and in Fig.3b the waves are propagating from the bottom of the image to the top. It is noted that in most cases, the velocities of the waves differ in the two different directions. Each image took around an hour to acquire, and the pixel size is $250\mu\text{m}$.

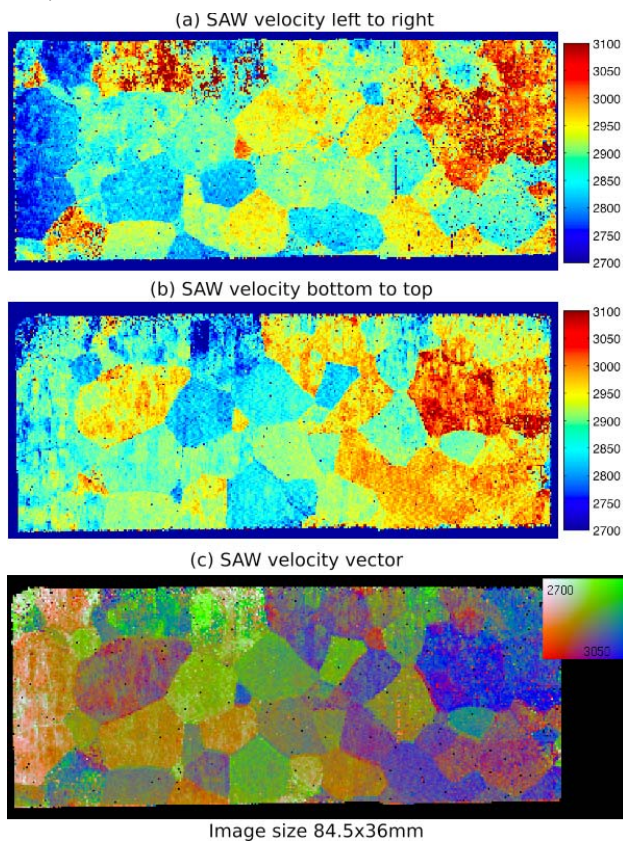


Fig.3. All three images in this figure are of the same sample of the titanium alloy known as Ti-6246, size 84.5 x 36mm. In (a), the SAWs are propagating from left to right; in (b) the SAWs are propagating from bottom to top. The different colours of (a) and (b) represent different SAW velocities, as denoted by the scale (in ms^{-1}) on the right of these sub-figures. (c) is a velocity vector image, combining the orthogonal velocity information of the previous two sub-figures. Here, the colours represent the relative velocities in both directions, as denoted by the colour-square on the right of (c).

The velocity vector map, shown in Fig.3c, is derived from the first two images as follows. First, the arrays of velocities are spatially matched using simple edge detection of the optical images, acquired at the same time as the acoustic information. In spatially matching the arrays, care is taken to offset the arrays by the propagation distance from the excitation source to the detection point, in the appropriate direction: remember that the SAW velocity corresponds to the area under the excitation region, not the detection point. Once the velocity arrays are correctly matched, a colour map is derived in which the colour of each point of the sample is determined by the SAW velocity in both directions. The colour scale could be anything of the user's choosing, and in the case of the velocity vector images presented in this paper, the colours are chosen according to the colour square on the right of Fig.3c. For example, if the velocity is "fast" in both directions, then the point will be coloured blue. If the velocity is "slow" in the horizontal direction and "fast" in the vertical direction, the point is coloured green. From this, excellent contrast between areas of different grain orientations is shown.

Fig.4 is of a different titanium alloy, known as Ti-685. Part (a) of the figure is an optical image of the sample, after it had been etched. As can be seen, the sample is in two parts. This is due to a load controlled low cycle fatigue fracture, and the failure process is described in detail in [9].

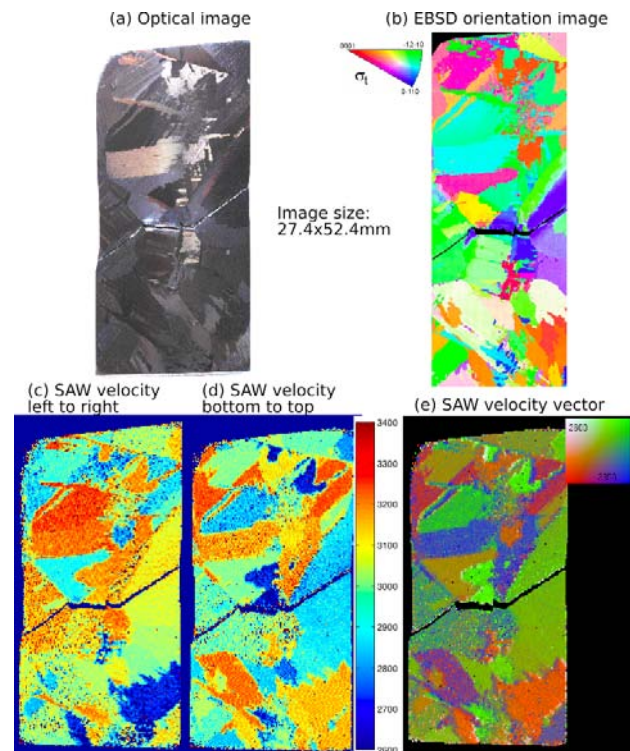


Fig.4. All images in this figure are of the same sample, a titanium alloy known as Ti-685. The SRAS images, (c), (d) and (e), are 27.4 x 52.4mm in size. (a) is an optical image of the sample, after it had been etched. The sample was then imaged using EBSD orientation imaging (b). (c) is a SAW velocity image, where the waves are propagating left to right; in (d), the waves are propagating bottom to top. (e) is the resulting SAW velocity vector image.

Fig.4b is an orientation image acquired using EBSD, where the different colours in the image represent different crystallographic orientations of the hexagonal close packed (hcp) α phase. Parts (c) and (d) are SAW velocity images, with waves propagating in the horizontal and vertical directions respectively, acquired using the SRAS technique. Fig.4e is the resulting SAW velocity vector image.

Striking similarities are noted, not only between the velocity vector image and the optical image, but more importantly between the EBSD orientation image and the velocity vector image. For instance, areas coloured red in the EBSD image correspond to the crystallographic orientation whereby the c-axis is parallel to the sample surface, and in the vertical direction (as one looks at the images). This corresponds to a relatively slow SAW velocity in the vertical direction, and a relatively fast velocity in the horizontal direction, which appears as a colour best described as "orangey-red" in the SAW velocity vector image. Similarly, areas where the velocity is relatively fast, and equal, in both directions, corresponds to crystals where the basal plane is parallel to the surface.

E. Conclusion

The spatially resolved acoustic spectroscopy technique described in this paper is a powerful, yet relatively simple, method of acquiring a map of material microstructure, using SAW velocity as its contrast mechanism. Furthermore, by combining two orthogonal velocity maps into a single velocity vector map, further information about the crystallographic orientation of grains can be deduced. Although much of the work linking SAW velocity in several directions to absolute orientation still remains to be done, the technique can already be used to determine certain unique orientations, such as when the basal plane of hcp crystals are parallel to the sample surface.

We have shown that SRAS and EBSD can be regarded as largely complimentary techniques. EBSD orientation imaging can produce outstandingly detailed images of true crystallographic orientation, with lateral resolution in the ten of nanometres scales. However, samples must be prepared by polishing to a mirror-like surface finish, and often the size of the sample is a limiting factor, as the sample is scanned at an angle of 70 degrees in a vacuum inside the scanning electron microscope used to acquire the EBSD images. It is also fair to say that good quality EBSD images can take a long time to acquire, and in practice it is this that limits the lateral resolution of images. SRAS, on the other hand, could be used on materials with no (or very little) surface preparation, and the size of the sample is limited only by the size of the scanning mechanism. For example, one can envisage a large scale system capable of imaging the surface of entire ingots of metals, several meters in size. Furthermore SRAS is relatively fast, is completely nondestructive, and is noncontact.

F. Acknowledgements

This work has been supported by the UK Research Centre for Non-Destructive Evaluation (RCNDE). The supply and heat treatment of the Ti-685 sample by Timet UK Research Labs is gratefully acknowledged.

G. Literature

- [1] M. R. Bache, "A review of dwell sensitive fatigue in titanium alloys: the role of microstructure, texture and operating conditions," *Int. J. Fatigue*, vol. 20, pp. 1079-1087, 2003.
- [2] C. F. Quate, "Acoustic microscopy: recollection," *IEEE Trans on Sonics and Ultrasonics*, vol. SU-32, p. 132, 1985.
- [3] R. S. Gilmore, "Ultrasonic Instruments and Devices II," in *Physical Acoustics* vol. 24. San Diego, CA, USA: Academic Press, 1999, pp. 275-346.
- [4] S. Sathish and R. W. Martin, "Quantitative imaging of Rayleigh wave velocity with a scanning acoustic microscope," *IEEE Trans. on Ultrasonics, Ferroelectrics and Frequency Control*, vol. 49, pp. 550-557, 2002.
- [5] S. Sathish, R. W. Martin and T. J. Moran, "Local surface skimming longitudinal wave velocity and residual surface stress mapping," *J. Acoust. Soc. Am.*, vol. 115, pp. 165-171, 2004.
- [6] S. D. Sharples, M. Clark and M. G. Somekh, "Fast noncontact imaging of material microstructure using local surface acoustic wave velocity mapping," *IEEE International Ultrasonics Symposium*, vols. 1-4, pp. 886-889, 2005.
- [7] S. D. Sharples, M. Clark and M. G. Somekh, "Spatially resolved acoustic spectroscopy for fast noncontact imaging of material microstructure," *Optics Express*, vol. 14, pp. 10435-10440, 2006.
- [8] S. D. Sharples, M. Clark and M. G. Somekh, "All-optical adaptive scanning acoustic microscope," *Ultrasonics*, vol. 41, pp. 295-299, 2003.
- [9] E. E. Sackett, L. Germain, and M. R. Bache, "Crystal plasticity, fatigue crack initiation and fatigue performance of advanced titanium alloys," *Int. J. Fatigue*, 2007, to be published.